

Reactivity of Organolanthanide Derivatives Containing the *o*-Aminothiophenolate Ligand toward Carbodiimide

Liping Ma, Jie Zhang,* Zhengxing Zhang, Ruifang Cai, Zhenxia Chen, and Xigeng Zhou*

Department of Chemistry, Fudan University, Shanghai 200433, People's Republic of China

Received June 5, 2006

A series of lanthanocene derivatives containing the *o*-aminothiophenolate ligand have been synthesized, and their reactivities toward carbodiimide have been investigated. Reaction of *N,N'*-diisopropylcarbodiimide (${}^i\text{PrN}=\text{C}=\text{N}^i\text{Pr}$) with $[\text{Cp}_2\text{Yb}(o\text{-H}_2\text{NC}_6\text{H}_4\text{S})]_2 \cdot 2\text{THF}$ ($\text{Cp} = \text{C}_5\text{H}_5$) (**1**) yields a centrosymmetric dimer, $[\text{Cp}(\text{THF})\text{Yb}(\mu\text{-}\eta^3\text{-}\eta^1\text{-SC}_6\text{H}_4\text{N}=\text{C}(\text{NH}^i\text{Pr})\text{N}^i\text{Pr})]_2$ (**2**), indicating that the adjacent NH_2 group can add to the $\text{C}=\text{N}$ double bonds of carbodiimide and one cyclopentadienyl group is eliminated. $[\text{Cp}_2\text{Dy}(o\text{-H}_2\text{NC}_6\text{H}_4\text{S})]_2 \cdot 3\text{THF}$, obtained by protolysis of Cp_3Ln with *o*-aminothiophenol, reacts with 2 or 1 equiv of ${}^i\text{PrN}=\text{C}=\text{N}^i\text{Pr}$ in THF at room temperature to give the partial amino group addition product $\text{CpDy}(\text{THF})[\mu\text{-}\eta^3\text{-}\eta^1\text{-SC}_6\text{H}_4\text{N}=\text{C}(\text{NH}^i\text{Pr})\text{N}^i\text{Pr}](\mu\text{-}\eta^2\text{-}\eta^1\text{-SC}_6\text{H}_4\text{NH}_2)\text{DyCp}_2 \cdot \text{THF}$ (**4**). When Cp_3Dy reacts with *o*-aminothiophenol, and subsequently with ${}^i\text{PrN}=\text{C}=\text{N}^i\text{Pr}$ in toluene at room temperature, we isolated complex **4** and a small amount of $[\text{Cp}_2\text{Dy}(o\text{-H}_2\text{NC}_6\text{H}_4\text{S})]_2 \cdot 2\text{THF}$ (**5**) and $[\text{Cp}(\text{THF})\text{Dy}(\mu\text{-}\eta^3\text{-}\eta^1\text{-SC}_6\text{H}_4\text{N}=\text{C}(\text{NH}^i\text{Pr})\text{N}^i\text{Pr})]_2$ (**6**). Treatment of 2 equiv of ${}^i\text{PrN}=\text{C}=\text{N}^i\text{Pr}$ with **3** in THF under reflux temperature also gave **4**; the residual NH_2 group cannot continuously add into the $\text{C}=\text{N}$ bonds of other carbodiimide molecules. Reaction of Cp_3Er with 2 equiv of *o*-aminothiophenol and subsequently with 2 equiv of ${}^i\text{PrN}=\text{C}=\text{N}^i\text{Pr}$ in THF at room temperature yields the bis-addition product $(\text{C}_5\text{H}_5)\text{Er}[\text{SC}_6\text{H}_4\text{NC}(\text{NH}^i\text{Pr})_2]_2$ (**7**). However, when Cp_3Er reacts with 2 equiv of *o*-aminothiophenol, and subsequently with 1 equiv of ${}^i\text{PrN}=\text{C}=\text{N}^i\text{Pr}$, the organic disulfide $({}^i\text{PrHN})_2\text{CNC}_6\text{H}_4\text{SSC}_6\text{H}_4\text{NC}(\text{NH}^i\text{Pr})_2$ (**8**) can be isolated. These results indicate that the addition of the adjacent amino group into the $\text{C}=\text{N}$ double bonds of the carbodiimide molecule is strongly affected by the metal ion character and the steric hindrance of the ligands. All of the new compounds have been characterized by elemental analysis and spectroscopic properties. Their structures have also been determined through X-ray single-crystal diffraction analysis.

Introduction

The activity of organolanthanide derivatives on unsaturated organic small molecules is one of the important fields of organolanthanide chemistry,^{1–3} and insertion, one flourishing subdiscipline of this field, has been studied extensively in past decades.^{4–9} However, little is known about the ligand modifica-

tions in organolanthanide chemistry. In fact, construction of novel ligands through the addition of functional substituents with unsaturated organic molecules is an important strategy in transition metal chemistry. The rewards are practical applications to synthesis of organometallic derivatives and potential understanding of catalytic processes.¹⁰ Few of the organolanthanide complexes have ever been found to undergo analogous reactions.¹¹ This is because the central metal strongly interacts with many of the reactants employed to result in the cleavage of the

(1) Reviews: (a) Evans, W. J.; Davis, B. L. *Chem. Rev.* **2002**, *102*, 2119. (b) Zhou, X. G.; Zhu, M. *J. Organomet. Chem.* **2002**, *647*, 28. (c) Ferrence, G. M.; Takats, J. *J. Organomet. Chem.* **2002**, *647*, 84.

(2) (a) Kirillov, E.; Lehmann, C. W.; Razavi, A.; Carpentier, J. F. *Eur. J. Inorg. Chem.* **2004**, 943. (b) Beetstra, D. J.; Meetsma, A.; Hessen, B.; Teuben, J. H. *Organometallics* **2003**, *22*, 4372. (c) Voth, P.; Arndt, S.; Spaniol, T. P.; Okuda, J.; Ackerman, L. J.; Green, M. L. H. *Organometallics* **2003**, *22*, 65. (d) Kornienko, A. Y.; Emge, T. J.; Brennan, J. G. *J. Am. Chem. Soc.* **2001**, *123*, 11933. (e) Evans, W. J.; Fujimoto, C. H.; Ziller, J. W. *Organometallics* **2001**, *20*, 4529. (f) Evans, W. J.; Kozimor, S. A.; Nyce, G. W.; Ziller, J. W. *J. Am. Chem. Soc.* **2003**, *125*, 13831.

(3) (a) Molander, G. A.; Romero, J. A. C. *Chem. Rev.* **2002**, *102*, 2161, and references therein. (b) Hong, S. W.; Kawaoka, A. M.; Marks, T. J. *J. Am. Chem. Soc.* **2003**, *125*, 15878. (c) Hong, S. W.; Tian, S.; Metz, M. V.; Marks, T. J. *J. Am. Chem. Soc.* **2003**, *125*, 14768. (d) Molander, G. A.; Pack, S. K. *J. Org. Chem.* **2003**, *68*, 9214. (e) Gribkov, D. V.; Hultsch, K. C.; Hampell, F. *Chem. Eur. J.* **2003**, *9*, 4796. (f) Hultsch, K. C.; Hampell, F.; Wagner, T. *Organometallics* **2004**, *23*, 2601. (g) Hong, S.; Marks, T. J. *Acc. Chem. Res.* **2004**, *37*, 673.

(4) (a) Zhang, J.; Zhou, X. G.; Cai, R. F.; Weng, L. H. *Inorg. Chem.* **2005**, *44*, 716. (b) Ma, L. P.; Zhang, J.; Cai, R. F.; Chen, Z. X.; Weng, L. H.; Zhou, X. G. *J. Organomet. Chem.* **2005**, *690*, 4926. (c) Zhang, J.; Cai, R. F.; Weng, L. H.; Zhou, X. G. *Organometallics* **2004**, *23*, 3303. (d) Zhang, J.; Cai, R. F.; Weng, L. H.; Zhou, X. G. *Organometallics* **2003**, *22*, 5385. (e) Zhang, J.; Cai, R. F.; Weng, L. H.; Zhou, X. G. *J. Organomet. Chem.* **2003**, *672*, 94. (f) Zhang, J.; Ruan, R. Y.; Shao, Z. H.; Cai, R. F.; Weng, L. H.; Zhou, X. G. *Organometallics* **2002**, *21*, 1420.

(5) (a) Evans, W. J.; Miller, K. A.; Ziller, J. W. *Inorg. Chem.* **2006**, *45*, 424. (b) Evans, W. J.; Forrestal, K. J.; Ziller, J. W. *J. Am. Chem. Soc.* **1998**, *120*, 9273. (c) Evans, W. J.; Seibel, G. A.; Ziller, J. W.; Doedens, R. J. *Organometallics* **1998**, *17*, 2103.

(6) (a) Shen, Q.; Li, H.; Yao, C.; Yao, Y.; Zhang, L.; Yu, K. *Organometallics* **2001**, *20*, 3070. (b) Mao, L.; Shen, Q.; Xue, M.; Sun, J. *Organometallics* **1997**, *15*, 3711.

(7) Zhang, W. X.; Nishiura, M.; Hou, Z. M. *J. Am. Chem. Soc.* **2005**, *127*, 16788.

(8) (a) Li, Y. R.; Pi, C. F.; Zhang, J.; Zhou, X. G.; Chen, Z. X.; Weng, L. H. *Organometallics* **2005**, *24*, 1982. (b) Zhang, C. M.; Liu, R. T.; Zhou, X. G.; Chen, Z. X.; Weng, L. H.; Lin, Y. H. *Organometallics* **2004**, *23*, 3246.

(9) Zhang, J.; Ma, L. P.; Cai, R. F.; Weng, L. H.; Zhou, X. G. *Organometallics* **2005**, *24*, 738.

(10) (a) Hayashi, T. In *Ferrocenes*; Togni, A., Hayashi, T., Eds.; VCH: Weinheim, 1995; p 105. (b) Cardin, D. J.; Cetinkaya, B.; Doyle, M. J.; Lappert, M. F. *Chem. Rev.* **1972**, *72*, 545. (c) Chen, J. T. *Coord. Chem. Rev.* **1999**, *192*, 1143. (d) Cuenca, T.; Royo, P. *Coord. Chem. Rev.* **1999**, *195*, 447. (e) Trost, B. M.; Rhee, Y. H. *J. Am. Chem. Soc.* **2002**, *124*, 2528.

(11) (a) Schumann, H.; Heim, A.; Demtschuk, J.; Mühle, S. H. *Organometallics* **2003**, *22*, 118. (b) Evans, W. J.; Perotti, J. M.; Brady, J. C.; Ziller, J. W. *J. Am. Chem. Soc.* **2003**, *125*, 5204. (c) Evans, W. J.; Brady, J. C.; Ziller, J. W. *J. Am. Chem. Soc.* **2001**, *123*, 7711.

lanthanide–ligand bond as more facile reaction pathways. Therefore the selective modification of ligands is an interesting and challenging task in organolanthanide chemistry.

Now our interest is the investigation on the reactivity of the functional substituted group of organolanthanide complexes to unsaturated organic small molecules. Recently, during the course of our investigation into the reaction of phenyl isocyanate with organolanthanide *o*-aminothiophenolate, we found that the neighboring NH₂ group can add to the residue C=N bond of the isocyanate insertion moiety to construct the thiazolate skeleton.⁹ The notable feature prompted us to explore the addition and expand it as a new method for the construction of the supporting ligands in organolanthanide chemistry. Furthermore, lanthanide-promoted (Lewis acid) nucleophilic addition of an organic amine RNH₂ to carbodiimide has been reported.¹² In this contribution, we reported the reactivity of lanthanocene complexes containing the *o*-aminothiophenolate ligand toward carbodiimide, which provides an efficient method for constructing a novel guanidinate anionic ligand by the amino group addition with the carbodiimide molecule accompanied with a 1,3-hydrogen shift and the abstraction of a cyclopentadienyl ring. Further investigations indicate that the selection of N–H bond addition and the abstraction of a Cp ring are strongly affected by the radii of the metal ions and/or the stoichiometric ratio of carbodiimide.

Experimental Section

General Procedure. All operations involving air- and moisture-sensitive compounds were carried out under an inert atmosphere of purified argon or nitrogen using standard Schlenk techniques. The solvents THF, toluene, and *n*-hexane were refluxed and distilled over sodium benzophenone ketyl under nitrogen immediately prior to use. (C₅H₅)₃Ln¹³ and [Cp₂Yb(*o*-H₂NC₆H₄S)]₂·2THF (**1**)⁹ were prepared by the literature methods. *N,N'*-Diisopropylcarbodiimide and *o*-aminothiophenol were purchased from Aldrich and were used without purification. Elemental analyses for C, H, and N were carried out on a Rapid CHN-O analyzer. Infrared spectra were obtained on a Nicolet FT-IR 360 spectrometer with samples prepared as Nujol mulls. Mass spectra were recorded on a Philips HP5989A instrument operating in EI mode. Crystalline samples of the respective complexes were rapidly introduced by the direct inlet techniques with a source temperature of 200 °C. The values of *m/z* refer to the isotopes ¹²C, ¹H, ¹⁴N, ¹⁶O, ¹⁶⁶Er, ¹⁶⁴Dy, and ¹⁷⁴Yb. ¹H NMR data were obtained on a Bruker DMX-500 NMR spectrometer.

Synthesis of [Cp(THF)Yb(μ-η³:η¹-SC₆H₄N=C(NHⁱPr)NⁱPr)]₂ (2**).** *N,N'*-Diisopropylcarbodiimide (0.141 g, 1.12 mmol) was slowly added to a 30 mL THF solution of **1** (0.559 g, 0.56 mmol) at room temperature, and the mixture was stirred for 24 h. The reaction solution was concentrated to ca. 5 mL by reduced pressure. Red crystals of **2** were obtained at –20 °C for several days. Yield: 0.439 g (70%). Anal. Calcd for C₄₄H₆₄N₆O₂S₂Yb₂: C 47.22, H 5.76, N 7.51. Found: C 47.21, H 5.83, N 7.71. IR (Nujol): 3383 m, 1591 w, 1570 m, 1534 s, 1424 s, 1064 m, 1033 s, 920 m, 774 s, 742 s, 598 w cm⁻¹. MS (70 eV): *m/z* (%) 488 (10) [1/2M – THF]. The CpH produced was identified by GC/MS.

Synthesis of [Cp₂Dy(*o*-H₂NC₆H₄S)]₂·3THF (3**).** (C₅H₅)₃Dy (0.450 g, 1.26 mmol) and *o*-aminothiophenol (0.158 g, 1.26 mmol) were mixed in 30 mL of THF. After stirring for 24 h at room temperature, all volatile substances were removed under vacuum to give a yellow powder. Pink crystals of **3** were obtained by recrystallization from THF at –20 °C for several days. Yield: 0.377

g (57%). Anal. Calcd for C₄₄H₅₆O₃N₂S₂Dy₂: C 50.32, H 5.37, N 2.67. Found: C 50.17, H 5.13, N 2.89. IR (Nujol): 3287 m, 3170 w, 1657 m, 1590 m, 1562 m, 1535 w, 1158 m, 1077 s, 1011 s, 906 m, 770 s, 681 m, 663 w cm⁻¹. MS (70 eV): *m/z* (%) 908 (3) [M – 2THF].

Synthesis of CpDy(THF)[μ-η³:η¹-SC₆H₄N=C(NHⁱPr)NⁱPr)]-(μ-η²:η¹-SC₆H₄-NH₂)DyCp₂·THF (4**).** *N,N'*-Diisopropylcarbodiimide (0.134 g, 1.06 mmol) was slowly added to a 30 mL THF solution of **3** (0.557 g, 0.53 mmol) at room temperature, and the mixture was stirred for 24 h. The reaction solution was concentrated to ca. 5 mL by reduced pressure. Pale yellow crystals of **4** were obtained at –20 °C for several days. Yield: 0.396 g (72%). Anal. Calcd for C₄₂H₅₆N₄O₂S₂Dy₂: C 48.60, H 5.44, N 5.40. Found: C 48.40, H 5.57, N 5.33. IR (Nujol): 3409 m, 3201 w, 3163 w, 1593 s, 1568 s, 1528 s, 1427 m, 1080 m, 1031 s, 919 m, 762 s, 731 s, 680 w, cm⁻¹. MS (70 eV): *m/z* (%) 644 (18) [M – 2THF – L] (L = SC₆H₄N=C(NHⁱPr)NⁱPr).

Synthesis of CpDy(THF)[μ-η³:η¹-SC₆H₄N=C(NHⁱPr)NⁱPr)]-(μ-η²:η¹-SC₆H₄-NH₂)DyCp₂·THF (4**), [Cp₂Dy(*o*-H₂NC₆H₄S)]₂·2THF (**5**), and [Cp(THF)Dy(μ-η³:η¹-SC₆H₄N=C(NHⁱPr)NⁱPr)]₂ (**6**).** (C₅H₅)₃Dy (0.583 g, 1.63 mmol) and *o*-aminothiophenol (0.204 g, 1.63 mmol) were mixed in 30 mL of toluene. After stirring for 48 h at room temperature, *N,N'*-diisopropylcarbodiimide (0.206 g, 1.63 mmol) was added into the solution. After stirring for 48 h, all volatile substances were removed under vacuum to give an orange powder. Pale yellow crystals of **4** were obtained at –20 °C for several days. Yield: 0.506 g (61%). Further crystallization by diffusion of *n*-hexane into the above mother liquor yielded purple crystals of **5**. Yield: 0.110 g (14%). Anal. Calcd for C₄₀H₄₈O₂N₂S₂Dy₂: C 49.13, H 4.95, N 3.09. Found: C 48.34, H 4.83, N 3.18. IR (Nujol): 3289 m, 3170 w, 1591 m, 1563 m, 1271 w, 1060 m, 1012 s, 910 s, 848 w, 779 w cm⁻¹. MS (70 eV): *m/z* (%) 836 (34) [M – 2THF]. Trace amounts of the purple crystals of **6** were obtained from the mother liquor at –20 °C for several days. IR (Nujol): 3371 m, 1590 w, 1574 m, 1533 s, 1421 s, 1060 m, 1030 s, 933 m, 770 s, 741 s, 596 w cm⁻¹. MS (70 eV): *m/z* (%) 478 (22) [1/2M – THF]. The amounts of **6** are too small to be characterized by elemental analysis.

Synthesis of (C₅H₅)₃Er[SC₆H₄NC(NHⁱPr)₂] (7**).** (C₅H₅)₃Er (0.522 g, 1.44 mmol) and *o*-aminothiophenol (0.361 g, 2.88 mmol) were mixed in 20 mL of THF. After stirring for 48 h at room temperature, *N,N'*-diisopropylcarbodiimide (0.364 g, 2.88 mmol) was added into the solution. After stirring for 48 h, all volatile substances were removed under vacuum to give an orange powder. Pink crystals of **7** were obtained by recrystallization from THF at –20 °C for several days. Yield: 0.893 g (77%). Anal. Calcd for C₃₅H₃₃N₆O₂Er: C 52.21, H 6.63, N 10.44. Found: C 52.04, H 6.63, N 10.53. IR (Nujol): 3413 s, 3203 w, 3050 m, 1594 s, 1568 s, 1529 s, 1427 s, 1029 s, 882 m, 774 s, 735 s cm⁻¹. MS (70 eV): *m/z* (%) 803 (13) [M].

Synthesis of (PrHN)₂CNC₆H₄SSC₆H₄NC(NHⁱPr)₂ (8**).** (C₅H₅)₃-Er (0.446 g, 1.23 mmol) and *o*-aminothiophenol (0.308 g, 2.46 mmol) were mixed in 20 mL of THF. After stirring for 48 h at room temperature, *N,N'*-diisopropylcarbodiimide (0.155 g, 1.23 mmol) was added into the solution. After stirring for 48 h, all volatile substances were removed under vacuum to give an orange powder. Colorless crystals of **9** were obtained by recrystallization from THF at –20 °C for several days. Yield: 0.222 g (37% based on *N,N'*-diisopropylcarbodiimide). Anal. Calcd for C₂₆H₄₀N₆S₂: C 62.37, H 8.06, N 16.79. Found: C 60.48, H 7.93, N 16.92. IR (Nujol): 3408 m, 3367 m, 1600 s, 1573 s, 1536 m, 1259 m, 1064 m, 1032 m, 856 w cm⁻¹. ¹H NMR (DCCl₃): δ 6.78–7.47 (m, 8H, C6H4), 3.85 (b, 4H, NHCH(CH₃)₂), 3.65 (m, 4H, NHCH(CH₃)₂), 1.22–1.57 (b, 24H, NHCH(CH₃)₂). MS (70 eV): *m/z* (%) 500 (38) [M].

X-ray Data Collection, Structure Determination, and Refinement. Suitable single crystals of complexes **2–8** were sealed under

(12) Yamamoto, N.; Isobe, M. *Chem. Lett.* **1994**, 2299.

(13) Magin, R. E.; Manastyrskij, S.; Dubeck, M. *J. Am. Chem. Soc.* **1963**, *85*, 672.

Table 1. Crystal and Data Collection Parameters of Complexes 2, 3, and 4

	2	3	4
formula	C ₄₄ H ₆₄ N ₆ O ₂ S ₂ Yb ₂	C ₄₄ H ₅₆ N ₂ O ₃ S ₂ Dy ₂	C ₄₂ H ₅₆ N ₄ O ₂ S ₂ Dy ₂
molecular weight	1119.21	1050.03	1038.04
cryst color	red	pink	pale yellow
cryst dimens (mm)	0.25 × 0.20 × 0.20	0.40 × 0.20 × 0.15	0.60 × 0.45 × 0.45
cryst syst	monoclinic	monoclinic	monoclinic
space group	<i>P</i> 2(1)/ <i>n</i>	<i>P</i> 2(1)	<i>C</i> 2/ <i>c</i>
<i>a</i> (Å)	10.056(3)	10.605(5)	14.524(6)
<i>b</i> (Å)	11.698(4)	16.487(7)	19.149(7)
<i>c</i> (Å)	19.363(9)	12.692(6)	30.795(11)
β (deg)	93.428(4)	92.591(6)	96.285(5)
<i>V</i> (Å ³)	2273.8(12)	2216.9(17)	8514(6)
<i>Z</i>	2	2	10
<i>D</i> _c (g·cm ⁻³)	1.635	1.573	1.620
μ (mm ⁻¹)	4.221	3.477	3.620
<i>F</i> (000)	1116	1044	4128
radiation	Mo Kα	Mo Kα	Mo Kα
(λ = 0.710730 Å)			
temperature (K)	293.2	293.2	298.2
scan type	ω-2θ	ω-2θ	ω-2θ
θ range (deg)	2.03 to 25.01	1.61 to 25.01	1.77 to 25.01
<i>h, k, l</i> range	-10 ≤ <i>h</i> ≤ 11 -13 ≤ <i>k</i> ≤ 13 -23 ≤ <i>l</i> ≤ 13	-8 ≤ <i>h</i> ≤ 12 -17 ≤ <i>k</i> ≤ 19 -15 ≤ <i>l</i> ≤ 15	-17 ≤ <i>h</i> ≤ 17 -20 ≤ <i>k</i> ≤ 22 -25 ≤ <i>l</i> ≤ 36
no. of reflns measd	9266	9255	17 751
no. of unique reflns	3992 (<i>R</i> _{int} = 0.0274)	7421 (<i>R</i> _{int} = 0.0407)	7505 (<i>R</i> _{int} = 0.0390)
completeness to θ	99.9% (θ = 25.01)	99.7% (θ = 25.01)	99.8% (θ = 25.01)
refinement method	full-matrix least-squares on <i>F</i> ²	full-matrix least-squares on <i>F</i> ²	full-matrix least-squares on <i>F</i> ²
no. of data/restraints/params	3992/0/253	7421/1/470	7505/0/469
goodness-of-fit on <i>F</i> ²	1.070	0.998	1.045
final <i>R</i> indices [<i>I</i> > 2σ(<i>I</i>)]	<i>R</i> ₁ = 0.0301, <i>wR</i> ₂ = 0.0785	<i>R</i> ₁ = 0.0494, <i>wR</i> ₂ = 0.1205	<i>R</i> ₁ = 0.0389, <i>wR</i> ₂ = 0.0750
<i>R</i> indices (all data)	<i>R</i> ₁ = 0.0378, <i>wR</i> ₂ = 0.0835	<i>R</i> ₁ = 0.0605, <i>wR</i> ₂ = 0.1290	<i>R</i> ₁ = 0.0610, <i>wR</i> ₂ = 0.0819
largest diff peak and hole (e ⁻ ·Å ⁻³)	1.123 and -0.904	1.992 and -1.158	0.888 and -0.603

argon in Lindemann glass capillaries for X-ray structural analysis. Diffraction data were collected on a Bruker SMART Apex CCD diffractometer using graphite-monochromated Mo Kα (λ = 0.71073 Å) radiation. During the intensity data collection, no significant decay was observed. The intensities were corrected for Lorentz-polarization effects and empirical absorption with the SADABS program.¹⁴ The structures were solved by the direct method using the SHELXL-97 program.¹⁵ All non-hydrogen atoms were found from the difference Fourier syntheses. The H atoms were included in calculated positions with isotropic thermal parameters related to those of the supporting carbon atoms, but were not included in the refinement. All calculations were performed using the SHELXL program. A summary of the crystallographic data and selected experimental information are given in Tables 1 and 2.

Results and Discussions

Reactivity of [Cp₂Yb(*o*-H₂NC₆H₄S)]₂·2THF (1) toward Carbodiimide. Addition of 2 molar equiv of ⁱPrN=C=NⁱPr to the THF solution of [Cp₂Yb(*o*-H₂NC₆H₄S)]₂·2THF (Cp = C₅H₅) (1)⁹ at ambient temperature results in a direct N-H bond addition product, [Cp(THF)Yb(μ-η³:η¹-SC₆H₄N=C(NHⁱPr)-NⁱPr)]₂ (2), indicating that the adjacent NH₂ group undergoes immediately a tandem intermolecular addition/1,3-hydrogen shift/CpH elimination, to yield the novel dianionic guanidinate ligand [SC₆H₄N=C(NHⁱPr)NⁱPr]²⁻, as shown in Scheme 1.

The formation process of 2 is different from the mechanism of the reaction of 1 with phenyl isocyanate, where phenyl isocyanate first inserts into the Yb-S σ-bonds of 1, then the adjacent NH₂ group adds to the residual C=N bond to form a cyclization product.⁹ We found only the addition of the activated

N-H bonds of the NH₂ group to the C=N bonds of the carbodiimide molecule occurs; the Ln-S σ-bond is inert to the insertion of carbodiimide. This might be attributed to the differences of the activity between PhNCO and ⁱPrN=C=NⁱPr.⁴ Significantly, the guanidinate anions as support ligands have been extensively explored in inorganic and organometallic chemistry.¹⁶ They are usually synthesized by two strategies of metathesis or insertion.¹⁷ Our reaction is the first example of the construction of the guanidinate anion ligand by the direct addition of the NH₂ group ligand to the carbodiimide molecule. It should be noted that the reaction of *o*-aminothiophenol with carbodiimide cannot take place under mild conditions; only original materials and a small amount of cyclization product can be obtained, identified by GC/MS.¹⁸ The present C-N bond-forming and subsequent 1,3-hydrogen shift and CpH elimination reaction are unprecedented and provide an effective method for the construction of new support ligands in organolanthanide chemistry.

Complex 2 has been characterized by elemental analysis and standard spectroscopic analysis, which were in good agreement with the proposed structures. Its structure was also identified by X-ray single-crystal diffraction analysis, as shown in Figure

(16) (a) Bailey, P. J.; Pace, S. *Coord. Chem. Rev.* **2001**, *214*, 91. (b) Ong, T. G.; Yap, G. P. A.; Richeson, D. S. *Organometallics* **2002**, *21*, 2839. (c) Ong, T. G.; Wood, D.; Yap, G. P. A.; Richeson, D. S. *Organometallics* **2002**, *21*, 1. (d) Cotton, F. A.; Daniels, L. M.; Huang, P. L.; Murillo, C. *Inorg. Chem.* **2002**, *41*, 317. (e) Bazinet, P.; Wood, D.; Yap, G. P. A.; Richeson, D. S. *Inorg. Chem.* **2003**, *42*, 6225. (f) Duncan, A. P.; Mullins, S. M.; Arnold, J.; Bergman, R. G. *Organometallics* **2001**, *20*, 1808.

(17) (a) Lu, Z.; Yap, G. P. A.; Richeson, D. S. *Organometallics* **2001**, *20*, 706. (b) Aelits, S. L.; Coles, M. P.; Swenson, D. G.; Jordan, R. F. *Organometallics* **1998**, *17*, 3265. (c) Tin, M. K. T.; Yap, G. P. A.; Richeson, D. S. *Inorg. Chem.* **1999**, *38*, 998. (d) Giesbrecht, G. R.; Shafir, A.; Arbold, J. J. *Chem. Soc., Dalton Trans.* **1999**, 3601.

(18) Recently, an example of the reaction of amine with carbodiimide under drastic conditions to form guanidine has been reported: Ong, T. G.; Yap, G. P. A.; Richeson, D. S. *Organometallics* **2003**, *22*, 387.

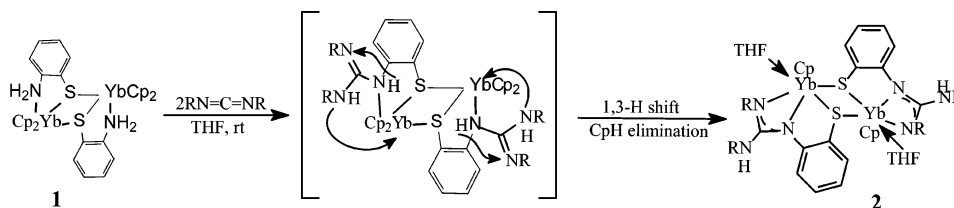
(14) Sheldrick, G. M. *SADABS*, A Program for Empirical Absorption Correction; Göttingen, Germany, 1998.

(15) Sheldrick, G. M. *SHELXL-97*, Program for the refinement of the crystal structure; University of Göttingen: Germany, 1997.

Table 2. Crystal and Data Collection Parameters of Complexes 5–8

	5	6	7	8
formula	C ₄₀ H ₄₈ N ₂ O ₂ S ₂ Dy ₂	C ₄₄ H ₆₄ N ₆ O ₂ S ₂ Dy ₂	C ₃₅ H ₅₃ N ₆ O ₂ Er	C ₂₆ H ₄₀ N ₆ S ₂
molecular weight	977.92	1100.15	805.21	500.76
cryst color	pale pink	purple	pink	colorless
cryst dimens (mm)	0.15 × 0.10 × 0.10	0.12 × 0.10 × 0.08	0.20 × 0.15 × 0.15	0.15 × 0.10 × 0.08
cryst syst	monoclinic	monoclinic	monoclinic	monoclinic
space group	<i>P</i> 2(1)/ <i>c</i>	<i>P</i> 2(1)/ <i>n</i>	<i>P</i> 2(1)/ <i>n</i>	<i>P</i> 2(1)/ <i>c</i>
<i>a</i> (Å)	10.986(3)	10.086(4)	16.236(8)	8.8220(11)
<i>b</i> (Å)	10.686(2)	11.719(4)	14.542(7)	16.951(2)
<i>c</i> (Å)	17.002(5)	19.487(7)	16.236(8)	19.423(2)
β (deg)	103.967(4)	93.451(4)	98.828(4)	100.784(2)
<i>V</i> (Å ³)	1937.0(9)	2299.2(14)	3788(3)	2853.1(6)
<i>Z</i>	2	2	4	4
<i>D_c</i> (g cm ⁻³)	1.677	1.589	1.412	1.166
μ (mm ⁻¹)	3.971	3.357	2.360	0.211
<i>F</i> (000)	964	1104	1652	1080
radiation	Mo Kα	Mo Kα	Mo Kα	Mo Kα
(λ = 0.710730 Å)				
temperature (K)	293.2	293.2	298.2	298.2
scan type	ω-2θ	ω-2θ	ω-2θ	ω-2θ
θ range (deg)	1.91 to 26.01	2.03 to 27.01	1.65 to 26.01	2.13 to 25.01
<i>h, k, l</i> range	-13 ≤ <i>h</i> ≤ 11 -13 ≤ <i>k</i> ≤ 13 -19 ≤ <i>l</i> ≤ 20	-12 ≤ <i>h</i> ≤ 12 -9 ≤ <i>k</i> ≤ 14 -24 ≤ <i>l</i> ≤ 23	-15 ≤ <i>h</i> ≤ 20 -14 ≤ <i>k</i> ≤ 17 -19 ≤ <i>l</i> ≤ 20	-9 ≤ <i>h</i> ≤ 10 -19 ≤ <i>k</i> ≤ 20 -23 ≤ <i>l</i> ≤ 21
no. of reflns measd	8759	11 050	16 787	12 722
no. of unique reflns	3790 (<i>R</i> _{int} = 0.0430)	4978 (<i>R</i> _{int} = 0.0473)	7418 (<i>R</i> _{int} = 0.0688)	5030 (<i>R</i> _{int} = 0.0288)
completeness to θ	99.6% (θ = 26.01)	99.2% (θ = 27.01)	99.7% (θ = 26.01)	99.8% (θ = 25.01)
refinement method		full-matrix least-squares on <i>F</i> ²		
no. of data/restraints/ params	3790/0/217	4978/0/257	7418/0/406	5030/0/307
goodness-of-fit on <i>F</i> ²	0.854	0.909	0.971	1.034
final <i>R</i> indices [<i>I</i> > 2σ(<i>I</i>)]	<i>R</i> ₁ = 0.0345, <i>wR</i> ₂ = 0.0599	<i>R</i> ₁ = 0.0300, <i>wR</i> ₂ = 0.0607	<i>R</i> ₁ = 0.0501, <i>wR</i> ₂ = 0.0827	<i>R</i> ₁ = 0.0524, <i>wR</i> ₂ = 0.1332
<i>R</i> indices (all data)	<i>R</i> ₁ = 0.0618, <i>wR</i> ₂ = 0.0643	<i>R</i> ₁ = 0.0431, <i>wR</i> ₂ = 0.0640	<i>R</i> ₁ = 0.1136, <i>wR</i> ₂ = 0.0999	<i>R</i> ₁ = 0.0834, <i>wR</i> ₂ = 0.1528
largest diff peak and hole (e ⁻ Å ⁻³)	1.026 and -1.043	1.123 and -0.626	1.358 and -0.735	0.434 and -0.362

Scheme 1. A Possible Formation Process of Complex 1



1. Selected bond lengths and angles of **2** are listed in Table 3. The structural analysis results show that the adjacent amino

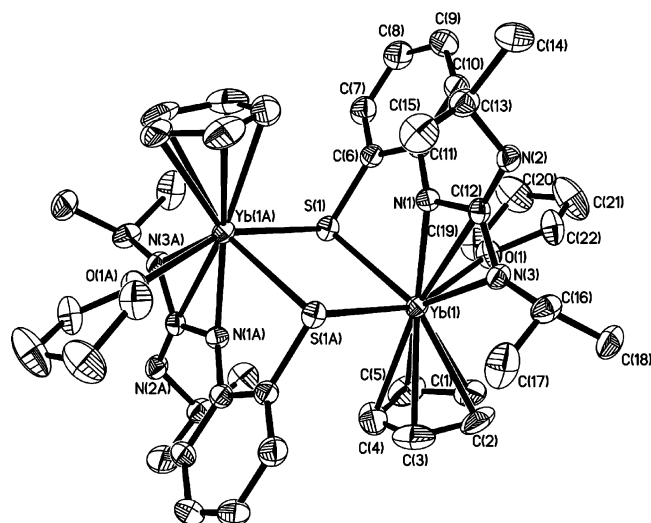


Figure 1. Thermal ellipsoid plot of [Cp(THF)Yb(μ-η³:η¹-SC₆H₄N=C(NH)Pr)N'Pr]₂, **2**, with ellipsoids at the 30% probability level.

Table 3. Selected Bond Lengths (Å) and Angles (deg) for **2**

Yb(1)–N(1)	2.273(4)	Yb(1)–S(1)	2.750(1)
Yb(1)–N(3)	2.344(4)	Yb(1)–C(12)	2.770(5)
Yb(1)–O(1)	2.447(4)	Yb(1)–S(1A)	2.798(2)
Yb(1)–C(5)	2.622(6)	S(1)–Yb(1A)	2.798(2)
Yb(1)–C(3)	2.628(7)	N(1)–C(12)	1.346(6)
Yb(1)–C(4)	2.632(7)	N(2)–C(12)	1.370(6)
Yb(1)–C(2)	2.640(6)	N(3)–C(12)	1.314(6)
Yb(1)–C(1)	2.642(6)		
N(1)–Yb(1)–N(3)	57.09(13)	N(3)–C(12)–N(2)	124.9(4)
S(1)–Yb(1)–S(1A)	82.80(4)	N(1)–C(12)–N(2)	123.0(4)
Yb(1)–S(1)–Yb(1A)	97.20(4)	N(3)–C(12)–Yb(1)	57.5(2)
C(12)–N(1)–Yb(1)	96.6(3)	N(1)–C(12)–Yb(1)	54.6(2)
C(12)–N(3)–Yb(1)	94.2(3)	N(2)–C(12)–Yb(1)	176.8(3)
N(3)–C(12)–N(1)	112.1(4)		

group in **2** has combined with *N,N'*-diisopropylcarbodiimide, forming a novel dianionic guanidinate ligand, [SC₆H₄N=C(NH)Pr)N'Pr]²⁻, which connects with the center metal by a novel μ-η³:η¹-bonding mode. One hydrogen atom of the adjacent amino group shifts to the uncoordinated nitrogen atom, similar to that of the unsymmetrical guanidinate complexes Cp₂Ln-[RNC(NH)Pr)N'Pr] (R = *t*Bu, Ln = Yb, Er, Dy; R = Ph, Ln = Yb).^{4c} The guanidinate ligand also exhibits delocalized bonding throughout the N₃C guanidinate core. The planarity of the YbN₂C ring and nearly equivalent C12–N1 and C12–N3

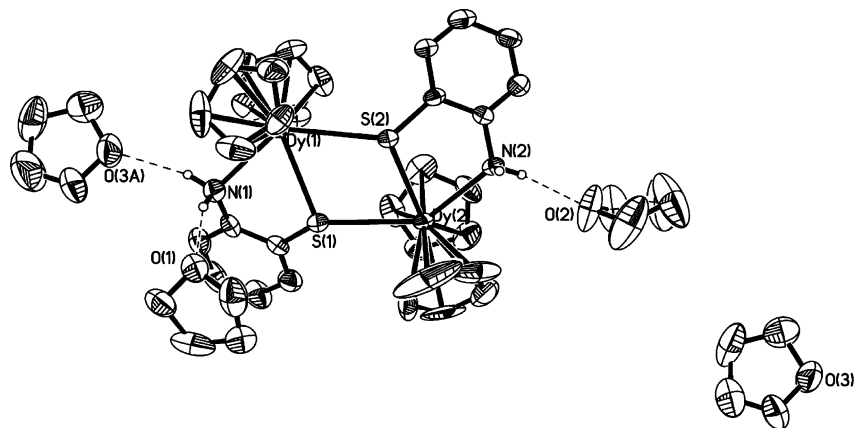
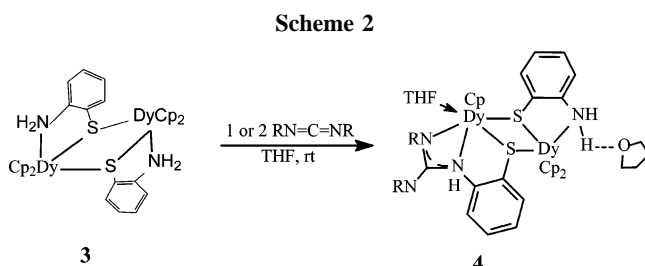


Figure 2. Thermal ellipsoid plot of $[\text{Cp}_2\text{Dy}(o\text{-H}_2\text{NC}_6\text{H}_4\text{S})]_2 \cdot 3\text{THF}$, **3**, with ellipsoids at the 30% probability level.



(1.346(6) and 1.314(6) Å, respectively) and Yb1–N1 and Yb1–N3 (2.273(4) and 2.344(4) Å, respectively) bond lengths suggest the existence of a resonance stabilization in the YbN_2C ring and no hydrogen atom at the coordinated nitrogen atom. The distance between the central carbon and uncoordinated nitrogen (C12–N2 1.370(6) Å) is significantly shorter than that expected for $\text{C}(\text{sp}^2)\text{--N}(\text{sp}^3)$ single bonds (C–N_{av}, 1.416 Å)¹⁹ and indicates a stronger $p\text{--}\pi$ conjugation between the lone-pair electron on noncoordinated nitrogen and the N–C–N unit. A weak interaction can be interpreted between the central carbon C(12) and the Yb^{3+} ion (Yb(1)–C(12) 2.770(5) Å).^{8c,9}

Reactivity of $[\text{Cp}_2\text{Dy}(o\text{-H}_2\text{NC}_6\text{H}_4\text{S})]_2 \cdot 3\text{THF}$ toward Carbodiimide. To further investigate the selectivity of the addition, we also synthesized the complex $[\text{Cp}_2\text{Dy}(o\text{-H}_2\text{NC}_6\text{H}_4\text{S})]_2 \cdot 3\text{THF}$ (**3**) by the reaction of Cp_3Dy with *o*-aminothiophenol in THF at room temperature and examined its reactivity toward *N,N'*-diisopropylcarbodiimide. The color of the crystal solid **3** is pink, different from that of other Cp_2Dy -containing compounds (pale yellow). Structural determination reveals an unsymmetrical intermolecular N–H \cdots O hydrogen-bonding mode in **3**, where one NH_2 group interacts with two THF molecules and the other amino group interacts with only one THF molecule (vide infra).

Reaction of **3** and 2 or 1 equiv of ${}^i\text{PrN}=\text{C}=\text{N}^i\text{Pr}$ in THF at room temperature gave the partial amino group addition product $\text{CpDy}(\text{THF})[\mu\text{-}\eta^3\text{:}\eta^1\text{-SC}_6\text{H}_4\text{N}=\text{C}(\text{NH}^i\text{Pr})\text{N}^i\text{Pr}][(\mu\text{-}\eta^2\text{:}\eta^1\text{-SC}_6\text{H}_4\text{NH}_2)\text{DyCp}_2 \cdot \text{THF}$ (**4**), as shown in Scheme 2, indicating that only one amino group adds to the carbodiimide molecule and the other amino group is retained. The residual NH_2 group also interacts with one THF molecule via an intermolecular N–H \cdots O hydrogen bond, confirmed by X-ray diffraction analysis. To identify the role of the intermolecular bond interaction, we also studied the reaction in toluene. When Cp_3Dy reacts with *o*-aminothiophenol in toluene at room temperature, and subsequently with ${}^i\text{PrN}=\text{C}=\text{N}^i\text{Pr}$, complex **4** and a small amount of $[\text{Cp}_2\text{Dy}(o\text{-H}_2\text{NC}_6\text{H}_4\text{S})]_2 \cdot 2\text{THF}$ (**5**) can be isolated, which is a

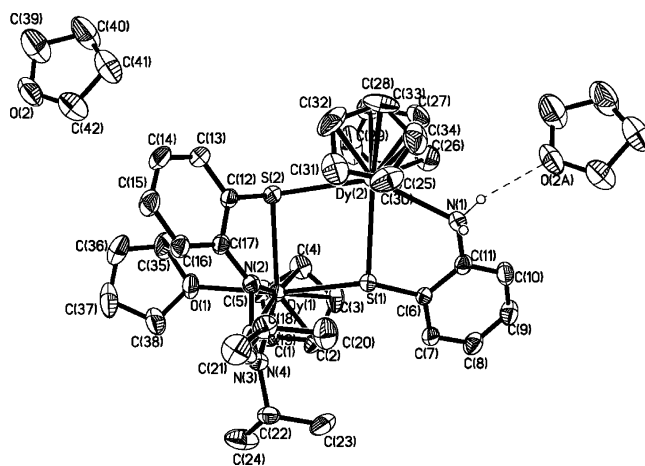


Figure 3. Thermal ellipsoid plot of $\text{CpDy}(\text{THF})[\mu\text{-}\eta^3\text{:}\eta^1\text{-SC}_6\text{H}_4\text{N}=\text{C}(\text{NH}^i\text{Pr})\text{N}^i\text{Pr}][(\mu\text{-}\eta^2\text{:}\eta^1\text{-SC}_6\text{H}_4\text{NH}_2)\text{DyCp}_2 \cdot \text{THF}$, **4**, with ellipsoids at the 30% probability level.

symmetric dimer geometry with two intermolecular hydrogen bond interactions, confirmed by X-ray single-crystal diffraction analysis. Further crystallization from the above mother liquor at low temperature, producing trace amounts of purple crystals $[\text{Cp}(\text{THF})\text{Dy}(\mu\text{-}\eta^3\text{:}\eta^1\text{-SC}_6\text{H}_4\text{N}=\text{C}(\text{NH}^i\text{Pr})\text{N}^i\text{Pr})]_2$ (**6**), which is an amino group completed addition product, has also been observed. These results may indicate that the partial addition is mainly affected by the character/radii of the rare earth metal Dy^{3+} ions, not the intermolecular hydrogen bond interactions.

It should be noted that the reaction of **3** with 2 equiv of ${}^i\text{PrN}=\text{C}=\text{N}^i\text{Pr}$ in THF under reflux temperature also gave **4**; the residual NH_2 group cannot continuously add into the C=N bonds of other carbodiimide molecules. To obtain the structure similar to **4**, the reaction of **1** with **2** in a 1:1 ratio has also been investigated. However, this reaction cannot take place, only the original materials can be obtained.

All these new complexes are sensitive to air and moisture and are characterized by standard analysis technology. Their solid structures have been determined by X-ray single-crystal diffraction analysis. As shown in Figure 2, an interesting feature of the structure of **3** is the different N–H \cdots O hydrogen bond interactions between the chelating coordinated NH_2 group and the uncoordinated THF molecules, which cause the aberrance of the planar Dy1–S1–Dy2–S2 four-membered ring (the dihedral angle of the S1–Dy1–S2 and S1–Dy2–S2 planes is 153.8°). Consistent with this, the distances of the Dy1–S1 and Dy2–S1 bonds (2.778(5), 2.832(5) Å) are significantly shorter than those of the Dy2–S2 and Dy1–S2 bonds (2.824(5), 2.932(5) Å), respectively. These results are different from the

(19) Lide, D. R., Ed. *Handbook of Chemistry and Physics*; CRC Press: Boca Raton, FL, 1996.

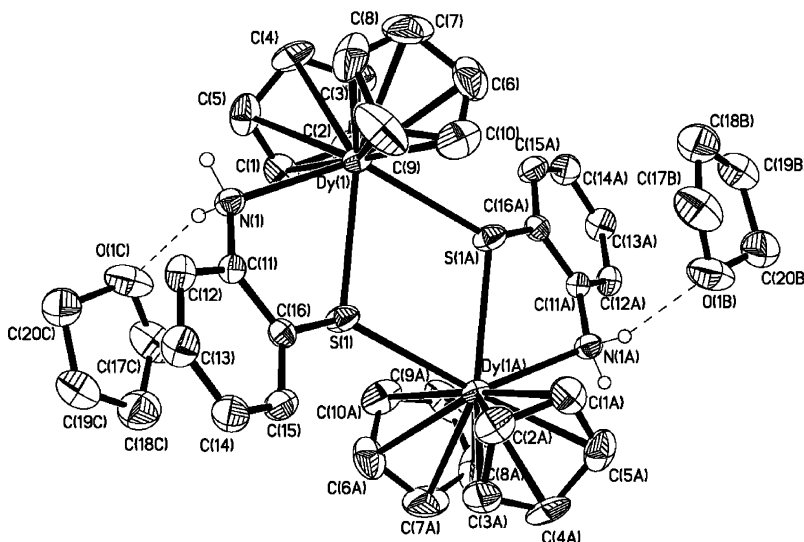


Figure 4. Thermal ellipsoid plot of $[\text{Cp}_2\text{Dy}(o\text{-H}_2\text{NC}_6\text{H}_4\text{S})]_2 \cdot 2\text{THF}$, **5**, with ellipsoids at the 30% probability level.

Table 4. Selected Bond Lengths (Å) and Angles (deg) for 3

Dy(1)–N(1)	2.508(11)	Dy(2)–C(23)	2.589(14)
Dy(1)–C(2)	2.610(16)	Dy(2)–C(26)	2.607(15)
Dy(1)–C(1)	2.614(18)	Dy(2)–C(19)	2.639(16)
Dy(1)–C(6)	2.645(15)	Dy(2)–C(24)	2.639(15)
Dy(1)–C(5)	2.652(14)	Dy(2)–C(18)	2.641(16)
Dy(1)–C(7)	2.652(18)	Dy(2)–C(21)	2.645(15)
Dy(1)–C(8)	2.661(14)	Dy(2)–C(25)	2.649(14)
Dy(1)–C(9)	2.663(14)	Dy(2)–C(20)	2.657(16)
Dy(1)–C(3)	2.679(15)	Dy(2)–C(17)	2.679(14)
Dy(1)–C(4)	2.678(13)	Dy(2)–S(2)	2.824(3)
Dy(1)–C(10)	2.693(15)	Dy(2)–S(1)	2.832(3)
Dy(1)–S(1)	2.778(3)	N(2)···O(2)	2.999(17)
Dy(1)–S(2)	2.932(3)	N(1)···O(3A)	2.98(2)
Dy(2)–N(2)	2.515(10)	N(1)···O(1)	2.970(18)
Dy(2)–C(22)	2.569(16)		
Dy(1)–S(1)–Dy(2)	111.08(10)	N(2)–H(2B)···O(2)	162.3(1)
Dy(2)–S(2)–Dy(1)	106.96(9)	N(1)–H(1B)···O(3A)	151.2(1)
S(1)–Dy(1)–S(2)	66.18(10)	N(1)–H(1A)···O(1)	157.7(1)
S(1)–Dy(2)–S(2)	66.96(9)		

observations of **1** or **5**, in which the symmetrical intermolecular hydrogen bond interactions are obtained.⁹

Figure 3 shows that complex **4** has a unique unsymmetrical dinuclear structure, in which the CpDy and Cp_2Dy fragments connect with the $[\text{SC}_6\text{H}_4\text{N}=\text{C}(\text{NH}^i\text{Pr})\text{N}^i\text{Pr}]^{2-}$ and $[\text{SC}_6\text{H}_4\text{NH}_2]^-$ units. The dianionic guanidinate ligand also connects with two dysprosium ions in the $\mu\text{-}\eta^3\text{:}\eta^1\text{-}$ mode, similar to the observation in **2**. The residual NH_2 group retains the intermolecular $\text{N}\cdots\text{H}\cdots\text{O}$ hydrogen bond interaction with one uncoordinated THF molecule. The example of the mixed mono(cyclopentadienyl)-lanthanide and bis(cyclopentadienyl)lanthanide in one unit is rare, though many structures of lanthanide derivatives containing the cyclopentadienyl ligand have been reported.²⁰

Crystal structure analysis (Figure 4, Table 6) confirms that complex **5** is a centrosymmetric dimeric structure, with the *o*-aminothiophenolate ligand as both a bridging and side-on donating group. Each Dy atom is coordinated by two cyclopentadienyl rings, two bridging sulfur atoms, and one chelating nitrogen atom to form an edge-bridged tetrahedral geometry. The intermolecular $\text{N}\cdots\text{H}\cdots\text{O}$ hydrogen bond interactions between the chelating coordinated NH_2 group and the uncoordinated THF also is symmetric, similar to **1**.⁹

As shown in Figure 5, complexes **6** and **2** are isostructural. The structural parameters of **6** (Table 7) are very similar to those

Table 5. Selected Bond Lengths (Å) and Angles (deg) for 4

Dy(1)–N(2)	2.293(4)	Dy(2)–C(31)	2.644(8)
Dy(1)–N(4)	2.404(4)	Dy(2)–C(29)	2.659(8)
Dy(1)–O(1)	2.440(4)	Dy(2)–C(34)	2.666(8)
Dy(1)–C(2)	2.664(7)	Dy(2)–C(25)	2.681(8)
Dy(1)–C(1)	2.665(6)	Dy(2)–C(30)	2.683(8)
Dy(1)–C(5)	2.668(6)	Dy(2)–C(26)	2.684(8)
Dy(1)–C(3)	2.677(7)	Dy(2)–S(1)	2.817(2)
Dy(1)–C(4)	2.679(6)	S(1)–C(6)	1.766(6)
Dy(1)–S(2)	2.7834(17)	S(2)–C(12)	1.780(6)
Dy(1)–C(18)	2.793(6)	N(1)–C(11)	1.454(7)
Dy(1)–S(1)	2.8439(18)	N(2)–C(18)	1.342(7)
Dy(2)–N(1)	2.562(5)	N(3)–C(18)	1.375(7)
Dy(2)–C(28)	2.609(8)	N(4)–C(18)	1.319(7)
Dy(2)–C(33)	2.625(8)	N(1)···O(2A)	3.082(8)
Dy(2)–C(32)	2.627(8)	O(2A)···H(1B)	2.21
Dy(2)–C(27)	2.641(7)		
N(2)–Dy(1)–N(4)	56.41(16)	N(4)–C(18)–N(3)	124.1(5)
N(2)–Dy(1)–S(2)	70.03(12)	N(2)–C(18)–N(3)	122.7(5)
S(2)–Dy(1)–S(1)	80.21(5)	N(3)–C(18)–Dy(1)	171.5(4)
N(4)–C(18)–N(2)	113.3(5)	N(1)–H(1B)···O(2A)	163.4

Table 6. Selected Bond Lengths (Å) and Angles (deg) for 5

Dy(1)–N(1)	2.507(4)	Dy(1)–C(2)	2.662(6)
Dy(1)–C(6)	2.631(7)	Dy(1)–C(1)	2.688(6)
Dy(1)–C(8)	2.632(8)	Dy(1)–C(5)	2.696(6)
Dy(1)–C(10)	2.639(7)	Dy(1)–S(1)	2.7743(17)
Dy(1)–C(9)	2.641(7)	S(1)–C(16)	1.761(6)
Dy(1)–C(7)	2.643(8)	S(1)–Dy(1A)	2.8764(16)
Dy(1)–C(3)	2.644(6)	N(2)···O(1C)	3.016(7)
Dy(1)–C(4)	2.659(6)	O(1C)···H(1C)	2.15
N(1)–Dy(1)–S(1)	66.27(11)	C(11)–N(1)–Dy(1)	116.6(3)
C(16)–S(1)–Dy(1)	101.6(2)	C(16)–C(11)–N(1)	117.8(5)
C(16)–S(1)–Dy(1A)	131.9(2)	C(11)–C(16)–S(1)	117.4(4)
Dy(1)–S(1)–Dy(1A)	111.95(6)	N(1)–H(1C)···O(1C)	161.0

found in complex **2**; the complex has no unusual distances or angles in the Cp_2Dy unit. The Dy–N distances of 2.303(3) and 2.389(3) Å are similar to the corresponding distances in complex **2**, when the difference in the metal ionic radii is considered.²¹

Reactivity of $\text{CpEr}(o\text{-H}_2\text{NC}_6\text{H}_4\text{S})_2$ toward Carbodiimide. To extend the scope of the addition, reactions of $\text{CpEr}(o\text{-H}_2\text{NC}_6\text{H}_4\text{S})_2$ with 1 or 2 equiv of $i\text{PrN}=\text{C}=\text{N}^i\text{Pr}$ have also been studied. As shown in Scheme 3, reaction of Cp_3Er with 2 equiv of *o*-aminothiophenol in THF at room temperature, and subsequently with 2 equiv of $i\text{PrN}=\text{C}=\text{N}^i\text{Pr}$, yields the bis-addition product $(\text{C}_3\text{H}_5)\text{Er}[\text{SC}_6\text{H}_4\text{NC}(\text{NH}^i\text{Pr})_2]_2$ (**7**). Structural analysis

(20) Watson, P. L.; Tulip, T. H.; Williams, I. *Organometallics* **1990**, *9*, 1999.

(21) Shannon, R. D. *Acta Crystallogr.* **1976**, *A32*, 751.

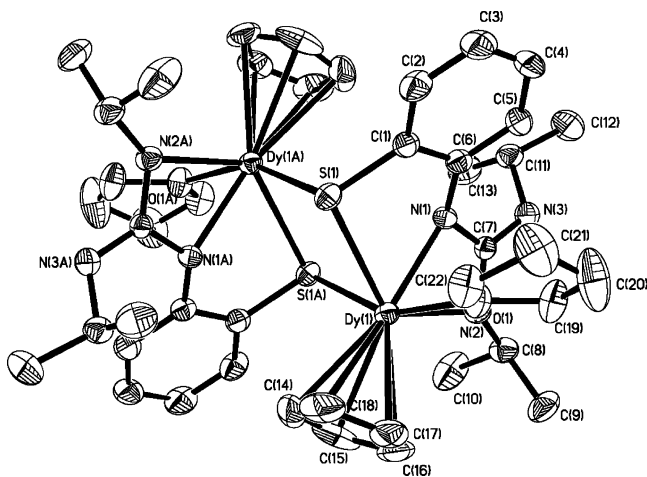
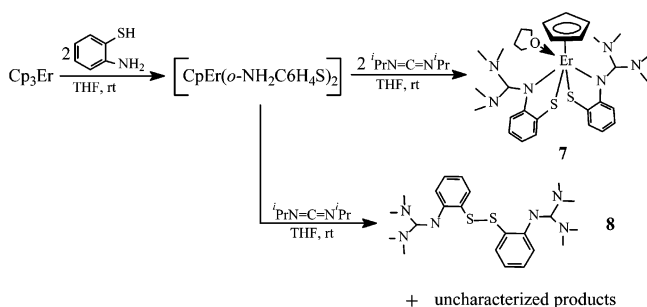


Figure 5. Thermal ellipsoid plot of $[\text{Cp}(\text{THF})\text{Dy}(\mu\text{-}\eta^3\text{:}\eta^1\text{-SC}_6\text{H}_4\text{N}=\text{C}(\text{NH}^i\text{Pr})\text{N}^i\text{Pr})_2]_2$, **6**, with ellipsoids at the 30% probability level.

Table 7. Selected Bond Lengths (Å) and Angles (deg) for 6

Dy(1)–N(1)	2.303(3)	Dy(1)–C(17)	2.686(5)
Dy(1)–N(2)	2.389(3)	Dy(1)–S(1)	2.797(1)
Dy(1)–O(1)	2.474(3)	Dy(1)–S(1A)	2.832(1)
Dy(1)–C(15)	2.665(5)	N(1)–C(7)	1.352(4)
Dy(1)–C(18)	2.669(5)	N(2)–C(7)	1.318(5)
Dy(1)–C(16)	2.677(5)	N(3)–C(7)	1.377(5)
Dy(1)–C(14)	2.679(5)		
N(1)–Dy(1)–N(2)	56.50(10)	C(7)–N(2)–Dy(1)	93.9(2)
N(1)–Dy(1)–S(1)	69.35(7)	N(2)–C(7)–N(1)	112.6(3)
N(2)–Dy(1)–S(1)	125.82(8)	N(2)–C(7)–N(3)	124.4(3)
S(1)–Dy(1)–S(1A)	83.29(3)	N(1)–C(7)–N(3)	122.9(3)
Dy(1)–S(1)–Dy(1A)	96.71(3)	N(3)–C(7)–Dy(1)	175.7(3)
C(7)–N(1)–Dy(1)	96.8(2)		

Scheme 3



reveals that both of the NH_2 groups add into the $\text{C}=\text{N}$ bonds of carbodiimide molecules, respectively, but no abstraction of cyclopentadienyl takes place. This may be attributed to the steric hindrance of the two guanidinate ligands $[\text{SC}_6\text{H}_4\text{NC}(\text{NH}^i\text{Pr})_2]^-$. However, when Cp_3Er reacts with 2 equiv of *o*-aminothiophenol, and subsequently with 1 equiv of $^i\text{PrN}=\text{C}=\text{N}^i\text{Pr}$, an organic disulfide, $(^i\text{PrHN})_2\text{CNC}_6\text{H}_4\text{SSC}_6\text{H}_4\text{NC}(\text{NH}^i\text{Pr})_2$ (**8**), was obtained. The residual solids are mixtures containing the metal ion Er^{3+} .

The X-ray analysis (Figure 6, Table 8) shows **7** is a solvated monomer, and the neutral guanidine group of the $[\text{SC}_6\text{H}_4\text{NC}(\text{NH}^i\text{Pr})_2]^-$ ligands is coordinated to the central metal with an η^1 -bonding mode. The erbium atom carries one η^5 -cyclopentadienyl group and one THF molecule and is chelated by two $[\text{SC}_6\text{H}_4\text{NC}(\text{NH}^i\text{Pr})_2]^-$ ligands. The coordination number of the central metal ion is eight. One important feature of the structure of **7** is that two $[\text{SC}_6\text{H}_4\text{NC}(\text{NH}^i\text{Pr})_2]^-$ ligands have distinctly different Er–N distances. The Er(1)–N(4) distance of 2.512(5) Å is significantly longer than the Er(1)–N(1) distance of 2.363(5) Å. This may

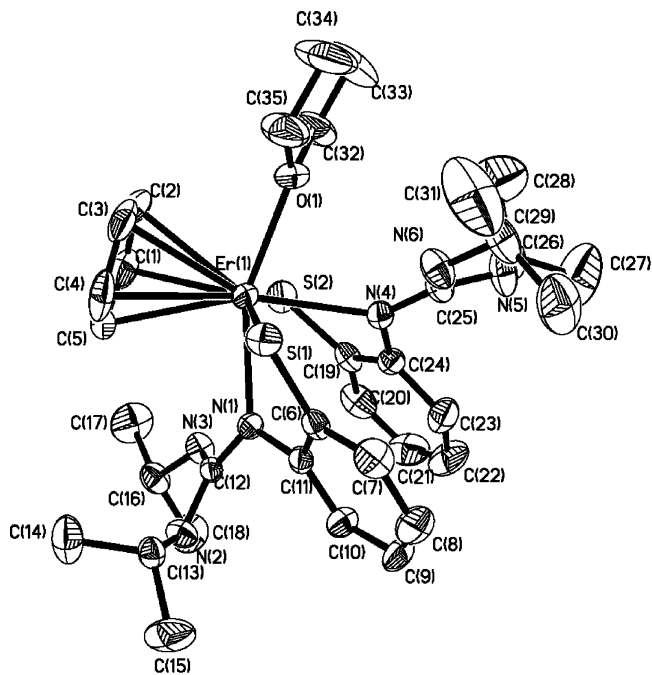


Figure 6. Thermal ellipsoid plot of $(\text{C}_5\text{H}_5)\text{Er}[\text{SC}_6\text{H}_4\text{NC}(\text{NH}^i\text{Pr})_2]_2 \cdot \text{THF}$, **7**, with ellipsoids at the 30% probability level.

Table 8. Selected Bond Lengths (Å) and Angles (deg) for 7

Er(1)–N(1)	2.363(5)	Er(1)–S(1)	2.735(2)
Er(1)–O(1)	2.385(5)	N(1)–C(12)	1.331(7)
Er(1)–N(4)	2.512(5)	N(2)–C(12)	1.341(8)
Er(1)–C(3)	2.650(8)	N(3)–C(12)	1.330(8)
Er(1)–C(2)	2.660(8)	N(4)–C(25)	1.337(8)
Er(1)–C(4)	2.666(8)	N(5)–C(25)	1.362(8)
Er(1)–C(1)	2.666(8)	N(6)–C(25)	1.310(8)
Er(1)–C(5)	2.687(8)	S(2A)···C(32)	3.641(9)
Er(1)–S(2)	2.730(2)	S(2A)···H(32A)	2.89
N(4)–Er(1)–S(2)	69.55(14)	N(6)–C(25)–N(4)	119.4(7)
N(1)–Er(1)–S(1)	73.17(14)	N(6)–C(25)–N(5)	116.6(7)
N(3)–C(12)–N(1)	118.1(6)	N(4)–C(25)–N(5)	124.0(7)
N(3)–C(12)–N(2)	117.3(6)	C(32)–H(32A)···S(2A)	134.7
N(1)–C(12)–N(2)	124.6(6)		

be attributed to the intermolecular $\text{S} \cdots \text{H} - \text{C}$ hydrogen bond interaction ($\text{S}(2\text{A}) \cdots \text{H}(32\text{A})$ 2.89 Å, $\text{S}(2\text{A}) \cdots \text{C}(32)$ 3.641(9) Å, $\text{S}(2\text{A}) \cdots \text{H}(32\text{A}) - \text{C}(32)$ 134.7°) and the large interligand steric interruption. Another important feature is that **7** exhibits completely delocalized bonding throughout the N_3C guanidine core. The distances of C(12)–N(1) (1.331(7) Å), C(12)–N(2) (1.341(8) Å), and C(12)–N(3) (1.330(8) Å) are approximately equivalent and are intermediate between the values observed for a C–N single bond distance and a C=N double bond distance. Consistent with this observation, the bond angles around the central carbon atom C(12) are almost 120° (N(1)–C(12)–N(2) 124.6(6)°, N(1)–C(12)–N(3) 118.1(6)°, N(3)–C(12)–N(2) 117.3(6)°). The bond angles around C(12) or C(25) are consistent with sp^2 hybridization (sum: 360°). These bond parameters indicate that the π -electrons of the C=N double bond are completely delocalized on the neutral guanidine groups. To our best knowledge, although many structures of organometallic complexes containing the neutral or anionic guanidinate ligands have been determined by X-ray diffraction analysis in the past decades, no example of the complete delocalization of π -electrons of the C=N double bond throughout the N_3C core has been reported. This can provide the possibility of synthesizing organometallic complexes containing Y-shaped guanidinate ligands such as the analogy of trimethylenemethane with the η^4 -bonding mode.²²

Table 9. Selected Bond Lengths (Å) and Angles (deg) for **8**^a

S(1)–C(13)	1.772(3)	C(18)⋯N(2)#1	3.542(4)
S(1)–S(2)	2.0290(11)	C(6)⋯N(5)#2	3.880(4)
S(2)–C(14)	1.787(3)	C(6)⋯N(6)#2	3.804(4)
C(7)–N(3)	1.297(4)	C(3)⋯N(4)#3	3.398(4)
C(7)–N(1)	1.358(3)	N(2)⋯N(4)#3	3.527(3)
C(7)–N(2)	1.360(3)	N(5)⋯N(3)#4	3.427(3)
C(20)–N(4)	1.289(3)	N(5)⋯S(1)#4	3.563(2)
C(20)–N(5)	1.360(3)	N(6)⋯N(3)#4	3.154(3)
C(20)–N(6)	1.363(3)		
C(13)–S(1)–S(2)	105.69(10)	C(18)–H(H18A)⋯N(2)#1	121.4
C(14)–S(2)–S(1)	106.08(10)	C(6)–H(6A)⋯N(5)#2	156.2
N(3)–C(7)–N(1)	123.3(3)	C(6)–H(6A)⋯N(6)#2	151.9
N(3)–C(7)–N(2)	120.2(3)	C(3)–H(3A)⋯N(4)#3	169.9
N(1)–C(7)–N(2)	116.5(3)	N(2)–H(2D)⋯N(4)#3	172.2
N(4)–C(20)–N(5)	119.1(2)	N(5)–H(5D)⋯N(3)#4	143.7
N(4)–C(20)–N(6)	127.7(2)	N(5)–H(5D)⋯S(1)#4	150.6
N(5)–C(20)–N(6)	113.2(2)	N(6)–H(6B)⋯N(3)#4	139.4

^a Symmetry transformations used to generate equivalent atoms: #1 $-x, y-1/2, -z+1/2$; #2 $x-1, y, z$; #3 $-x, y+1/2, -z+1/2$; #4 $x+1, y, z$.

The disulfide **8** was proven by the X-ray analysis. Selected bond distances and bond angles are compiled in Table 9. It can be seen (Figure 7) that the molecular structure of **8** confirms the amino group addition to the C=N bonds of carbodiimide molecules. The formed guanidine groups display only partial delocalization of the π -electrons of the C=N bond on the N₃C core. The distances of C(7)–N(3) (1.297(4) Å) or C(20)–N(4) (1.289(3) Å) double bonds are comparable to the accepted value for the N(sp²)=C(sp²) double bond (1.28 Å).²³ The length of the S–S bond is 2.029(1) Å and in the normal range. There are eight kinds of intramolecular or intermolecular hydrogen-bonding interactions in the crystal packing of **8**, which assemble a one-dimension helical chain structure.

Conclusions

The present results demonstrate that bis(cyclopentadienyl)-lanthanide complexes containing the *o*-aminothiophenolate

(22) Ando, W.; Yamamoto, T.; Saso, H.; Kabe, Y. *J. Am. Chem. Soc.* **1991**, *113*, 2791.

(23) March, J. In *Advanced Organic Chemistry*; McGraw-Hill: New York, 1997; Vol. 2, p 24.

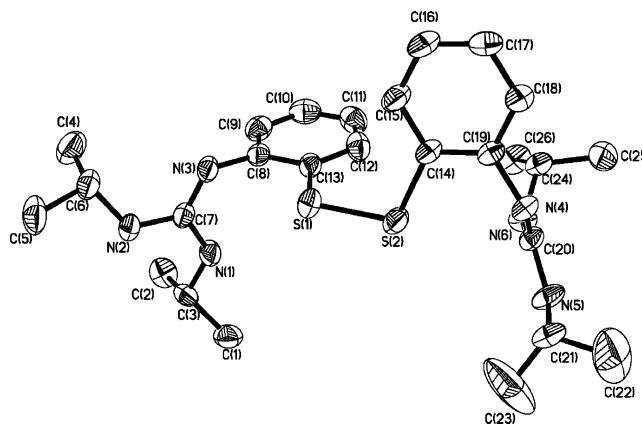


Figure 7. Thermal ellipsoid plot of (iPrHN)₂CNC₆H₄SSC₆H₄NC(NHPr)₂, **8**, with ellipsoids at the 30% probability level.

ligand exhibit high activity toward carbodiimide. The N–H bonds of the adjacent amino group can selectively add to the C=N bond of the carbodiimide molecule and provide effective methods for construction of the novel dianionic [SC₆H₄N=C(NHR)NR]²⁻ or monoanionic [SC₆H₄N=C(NHR)₂]⁻ guanidinate ligands. Further study indicates that the selectivity of the adjacent amino group addition to C=N bonds of carbodiimide or abstraction of a Cp ring can be affected by metal ionic character/radii and/or the stoichiometric ratio of carbodiimide. These reactions introduce a new strategy to synthesize novel organolanthanide derivatives via ligand modifications. Further investigations into the formation mechanism of **8** and the reactivity of these complexes are underway.

Acknowledgment. We thank the National Natural Science Foundation of China and the Research Funds of Young Teacher of Fudan University for financial support.

Supporting Information Available: Tables of atomic coordinates and thermal parameters, all bond distances and angles, and experimental data for all structurally characterized complexes. This material is available free of charge via the Internet at <http://pubs.acs.org>.

OM060491H